Developing Pediatric ATD Thoracic Biofidelity Requirements from Cardiopulmonary Resuscitation Data

T. Castner[1], K. B. Arbogast[2,3], V. Nadkami[2,4], R. Sutton[2], A. Nishisaki[2], M. R. Maltese[2]
[1]University of Pennsylvania, [2]The Children's Hospital of Philadelphia, [3]Department of Pediatrics, The University of Pennsylvania, [4]University of Pennsylvania School of Medicine

ABSTRACT

Obtaining accurate pediatric thoracic force-deflection characteristics is critical for the development of biofidelic pediatric anthropometric test devices (ATD) used in designing motor vehicle crash safety systems. Owing to the paucity of pediatric post-mortem human subjects (PMHS) for research, such characteristics in modern pediatric ATD's are based on scaled adult PMHS data. However, such scaling processes give limited consideration to the tissue and morphological differences associated with human maturation. In the clinical setting, the magnitude of chest compressions on pediatric subjects undergoing cardiopulmonary resuscitation (CPR) are in the range of chest deflection limits in Federal frontal crash test regulations. Thus, the goal of this study is to describe analytical methods and preliminary data from 19 CPR Events, towards a biofidelity design standard for the pediatric ATD thorax. A novel force and deflection sensor has been integrated into a clinical monitor-defibrillator used during CPR at the Children's Hospital of Philadelphia. The sensor is interposed between the chest and hands during CPR compressions, and is designed to provide real-time feedback to improve the quality of CPR. Thoracic force and compression data are downloaded from the monitor-defibrillator for analysis following a CPR event. Each compression is fit to a parallel spring-damper model, wherein stiffness and damping are linearly dependant on depth. Nineteen CPR events were recorded, consisting of 31,535 compressions. Maximum applied force ranged from 37 N to 613 N, chest compressions from 15 mm to 76 mm, and compression velocity from 0.044 m/s to 0.64 m/s. Analysis of these data is ongoing. This study provides a promising method with which to measure the biomechanical properties of a live pediatric thorax, with the potential to improve the accuracy of pediatric ATD's.

INTRODUCTION

Pediatric anthropometric test devices (ATD) are a key tool for developing motor vehicle safety systems. Such ATDs, including the Hybrid III family and Q series, are limited by the adult-derived biofidelity data used to guide their design. That is, the design requirements that ensure the child ATD behaves like a human during an impact (generally termed "Biofidelity" requirements) are based upon size-scaled data from adult cadaver and adult volunteer impact experiments. Due to the sparse pediatric biomechanical data available at the time these ATD's were developed, these scaling efforts had minimal consideration for the differences in anatomy and material properties between adults and children. However, in order to reduce the 1638 child occupants aged 0 to 14 who died in 2004 in the US, 50% of whom were restrained (NHTSA, 2004), advances to the state of the art of pediatric ATDs are required. Through funding from NHTSA, The Center for Injury Research and Prevention at the Children's Hospital of Philadelphia has developed the capability to extract thoracic force vs. deflection data, at crash-relevant deflections, from pediatric clinical patients undergoing cardiopulmonary resuscitation (CPR). Herein we describe a method to collect such thoracic force deflection data, and thus develop enhanced scaling factors towards a revised thoracic impact response requirement.

Influence of Anatomy and Material Properties on Mechanical Response

Previous efforts have characterized differences between pediatric and adult biomechanical properties in areas other than the thorax. Ching et al (2001) and Hilker et al (2002) conducted neck tensile stiffness and failure experiments on pediatric human-equivalent animal models. Similarly, studies of pediatric neck cadaver specimens have been published (Ouyang, 2005) or are underway (Prange, 2006) These studies document the significant difference in strength of whole anatomical regions between adult and child subjects, and how such strength is influenced by geometric and material differences.

Inspection of the torso maturation process yields an appreciation for amount time required for bones in the rib cage to appear and fuse. The sternum consists of 6 main bones – the manubrium superiorly, followed by sternebrae 1 through 4 and the xiphoid process. The 4th sternebra appears at age 12 months, while the xiphoid process appears at 3 to 6 years. Fusing between sternebrae begins at age 4 years and continues through age 20 years (Figure 1). The sternum as a whole descends with respect to spine from birth up until age 2 to 3 years, causing the ribs to angle downward when viewed laterally, and the shaft of the rib to show signs of axial twist deformation (Scheuer, 2000). The costal cartilage also calcifies with age, likely influencing its flexibility (Figure 1). Thus, children differ from the adult not only geometrically, but materially and structurally, and these differences likely influence the mechanical response of the child to blunt impact.

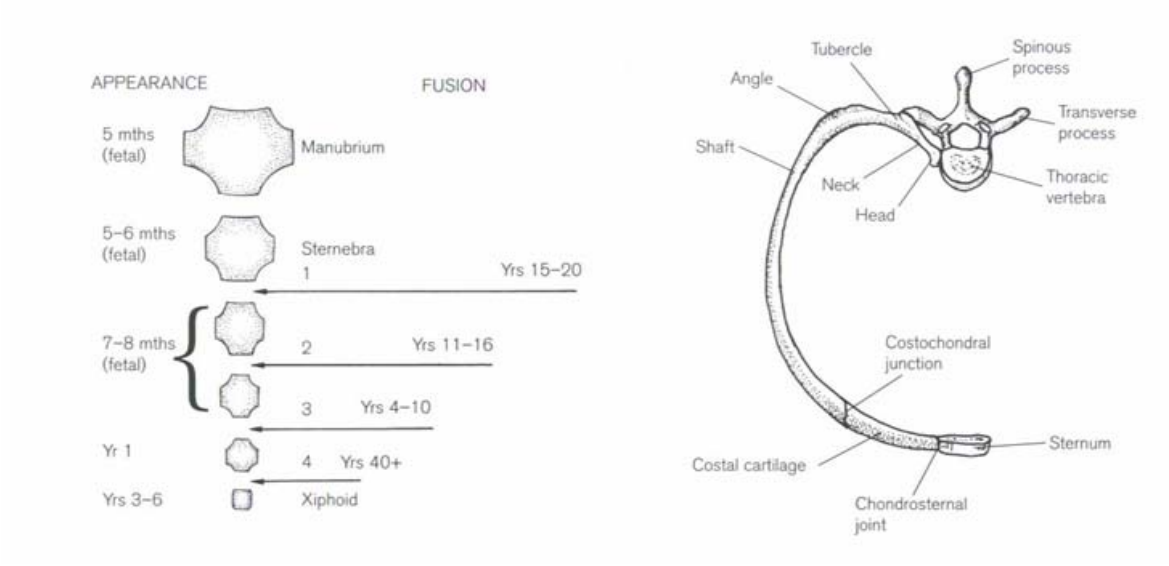

Figure 1: Development of the sternum (left) and the typical thoracic rib (right).
(Reprinted from Scheuer, 2000)

Adult-to-child scaling of ATD Biofidelity Requirements

Irwin et al (1997) developed impact corridors for pediatric crash test dummies. For the chest, the authors used the ubiquitous Kroell (Kroell, 1974) thoracic impact tests, where an impactor with a constant initial velocity is propelled into the torso of cadavers. The authors applied equations that yield the ratio of the chest deflection and force between the adult and child,

$$R_D = \lambda_x \qquad R_F = \lambda_E \lambda_x \lambda_z$$

where λ_E is the ratio of the elastic moduli of skull bone, and λ_x and λ_z are the ratios of the characteristic lengths in the x and z directions, respectively.

Similarly, equations were developed that scale the mass of the impactor used in the test, and are also notably dependent upon elastic moduli of the thorax, with skull modulus used as a surrogate. The work of Irwin et al forms the basis for the Hybrid III family of child ATD's employed in Federal Motor Vehicle Safety Standard (FMVSS) No. 208 Frontal Impact Protection and No. 213 Child Restraint Evaluation in the United States, and similar standards in Canada. Others (Van Ratingen, 1997) have developed similar techniques to guide the design of European pediatric ATD's, and in the case of the thorax have employed femur elastic modulus. One theme runs throughout the cited scaling papers – thoracic material property parameters figured prominently in the scaling equations, and limited available pediatric data led the authors to use data from other body regions in place of thoracic material information.

In pursuit of thoracic material data to complete the equations above, efforts are underway at the Ohio State University (Bolte, 2006) to characterize the bending stiffness of pediatric rib.

These data are important in the development of finite element models of the human thorax, and will be useful in determining the role of the rib, costocartilage, costovertebral junction, and sternum in governance of thoracic deflection. The research proposed herein will serve as complement to the OSU rib data, as it investigates the impacted chest as a system and will thus extract the overall elastic modulus of the thorax.

Measuring Pediatric Thoracic Stiffness

Our research facility has procured a method for measuring the applied force and sternal deflection of the thorax during CPR. In brief, a load cell and accelerometer sensor package has been integrated into a clinical monitor-defibrillator (Laerdal Medical, Stavenger, Norway) to track chest compression and applied force during CPR. This Force Deflection Sensor (FDS) is interposed between the palms of the hands of the person administering CPR and the sternum of the patient. The accelerometer signal is processed with a double-integration algorithm, yielding deflection. The performance of the device was validated against optical deflection measurement systems. The development of this technology affords the opportunity to measure the force-deflection characteristics of the thorax from live humans. Of importance, during cardiac arrest, chest compliance is not confounded by muscle activity. The EEG becomes isoelectric within 15 to 20 seconds, and the patient becomes flaccid (Clark, 1992; Bang, 2003). Even involuntary muscle tone disappears within five minutes as measured in the esophageal sphincter (Bowman, 1995). Thus, the significance of the development of the FDS is that it provides the first means we are aware of to directly measure the force vs. deflection characteristics of the live pediatric chest to crash-relevant deflections without the effects of muscle tensing. The implication of knowing the force-vs-deflection characteristics is that it now becomes possible to confidently scale the thoracic deflection response from adult cadaver blunt impact tests (Kroell, 1974) or belt loading tests (Kent, 2004).

METHODS

Extracting the thoracic characteristics is subject to several constraints due to the clinical nature of the experiment as well numerical errors in data analysis. The numerical accuracy of the acceleration to deflection double integration has been documented to be fairly accurate, >1.3 mm error with 95% confidence (Aase, Myklebust, 2002), when performed on a rigid surface. However, the accelerometer in the FDS measures acceleration with respect to the ground and not with respect to the patient's spine; thus, when compressions are preformed on a non-rigid surface the deflection of the non-rigid surface must be accounted for. As this data is collected in the clinical setting the compressions are performed either on a bed or stretcher both of which are non-rigid. This correction is performed by comparing the force in the actual CPR event to that in reference case in which compressions are performed on a manikin, with the same thoracic mass as that of the patient, on the same bed. The thoracic characteristics are also subject to error due to the clinical nature of the experiment, as the state of health of the patients may affect the condition of the chest.

Data Collection

Data was collected from the Emergency Department (ED) and Pediatric Intensive Care Unit (PICU) of our hospital. Patients must be at least 8 years old in order to qualify for our study.

The force and acceleration data as measured by the FDS is collected by a clinical monitor/deliberator. Once the data has been collected and the event is completed, the bed or stretcher is tagged and held for later creation of a reference case in a CPR event reconstruction. The position of the backboard and patient are recorded as well as other information, including patient mass, height, age and estimated thoracic mass.

A reference case is then performed on the held and tagged bed. The CPR manikins are weighted to represent the mass of the patient's thorax, the position of the head board and patient are also recreated. A reference accelerometer is also placed in the spine of the CPR manikin.

The Chest/Mattress model

The model used to characterize the chest is a linear depth dependant spring and damper model. A depth independent stiffness (k_1) , depth dependant stiffness (k_2), depth independent damping (μ_1) and depth dependant damping (μ_2) are calculated such that:

(1) $$F_{chest} = x_{chest}\left(k_1 + x_{chest}k_2\right) + v_{chest}\left(\mu_1 + x_{chest}\mu_2\right)$$

where F_{chest} is the force exerted on the chest, x_{chest} is the deflection of the chest and v_{chest} is the rate of chest deflection. A similar model is used to determine the mattress characteristics, except the stiffness values are non-linear such that:

(2) $$F_{mattress} = x_{mattress}K_m\left(x_{mattress}\right) + v_{mattress}\left(\mu_1 + x_{mattress}\mu_2\right)$$

where $K_m\left(x_{mattress}\right)$ is the depth dependant stiffness function represented by a look-up table. $F_{mattress}$ and F_{chest} and $x_{mattress}$ and x_{chest} are related by the equations of motion according to Figure 2 and Equations 3 and 4:

(3) $$F_{chest} = F_{mattress} + Ma_{mattress} + m\left(a_{chest}\right)$$

(4) $$\iint a_{chest}dt = x_{mattress} + x_{chest}$$

where $a_{mattress}$ is the acceleration of the spine / mattress, a_{chest} is the acceleration of the sternum, m is the mass of components accelerating relative to the spine – this mass is considered negligible, and M is the mass of the rest of components accelerating relative to the ground – the estimated mass of the thorax is used here.

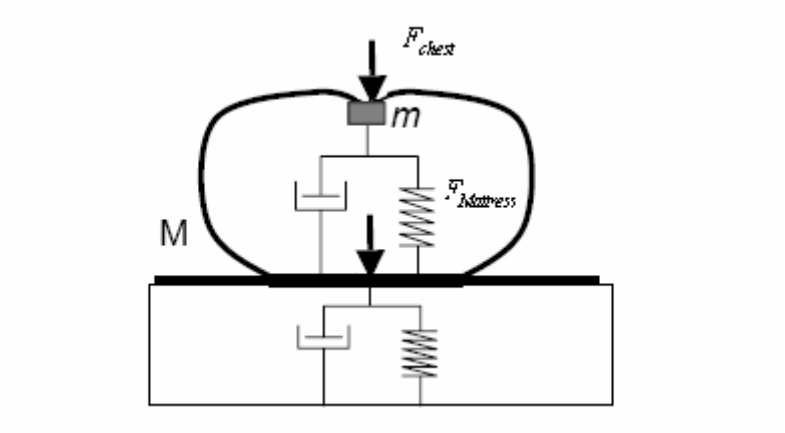

Figure 2: Mechanical model of chest atop non-ridged surface.

Mattress Correction

Combining equations 2 and 3 and assuming m is negligible:

(2) $$F_{mattress} = x_{mattress} K_m\left(x_{mattress}\right) + v_{mattress}\mu_m\left(x_{mattress}\right)$$

(3) $$F_{mattress} = F_{chest} - Ma_{mattress}$$

$$F_{chest} = x_{mattress} K_m\left(x_{mattress}\right) + v_{mattress}\mu_m\left(x_{mattress}\right) + Ma_{mattress}$$

(5) $$x_{mattress} = \frac{F_{chest} - Ma_{mattress} - v_{mattress}\mu_m\left(x_{mattress}\right)}{K_m\left(x_{mattress}\right)}$$

We however cannot solve equation 5 for $x_{mattress}$ as μ_m, K_m, $v_{mattress}$ and $a_{mattress}$ are all dependant on $x_{mattress}$. Instead an iterative method is used to estimate the solution to Equation 5. A fist order approximation is found by only solving based on a static model:

(6) $$x_{mattress1} = \frac{F_{chest}}{K_m\left(x_{mattress1}\right)}$$

Where $K_m\left(x_{mattress1}\right)$ is linear to $x_{mattress1}$, and thus solvable. A first order estimation of the velocity and acceleration is then found by taking gradients of the first order estimation of depth. This first order estimation is then used to calculate a second order estimation by solving for the dynamic model:

(7) $$x_{mattress2} = \frac{F_{chest} - M\left(\ddot{x}_{mattress1}\right) - \left(\dot{x}_{mattress1}\right)\mu\left(x_{mattress1}\right)}{K_m\left(x_{mattress2}\right)}$$

For further accuracy third order estimation is taken using the second order estimation to solve again for the dynamic model in equation 7. The data is filtered at the end of each estimation using a high order finite impulse response (FIR) filter, using a Kaiser Window with a passband frequency of 5 Hz, a stopband frequency of 6Hz, passband ripple of .5% and stopband ripple of 5%.

Data Analysis

For each compression of the corrected chest depths, the four values of the model (k_1, k_2, μ_1, μ_2) are calculated using the chest depth and the gradient of the chest depth according to equation 1. The model was only applied to part of the compression where the depths are greater than 10mm. To perform the calculation for the entire compression, an over defined matrix is created by solving Equation 1 for each data point. The over defined matrix is solved using Householder reflections to calculate an orthogonal-triangular factorization such that:

$$X_{chest} * P = Q * R_{chest} \tag{8}$$

where X_{chest} is an n x 4 matrix of chest conditions where the nth column is the row vector $\left\langle x_{chest}, x_{chest}^2, \dot{x}_{chest}, \dot{x}_{chest} x_{chest} \right\rangle$, P is the permutation matrix, Q is the orthogonal matrix and R_{chest} is the upper triangular. The least squares solution is computed such that:

$$\left\langle k_1, k_2, \mu_1, \mu_2 \right\rangle = P * \left(\frac{Q^T * B}{R} \right) \tag{9}$$

Each compression is evaluated for several criteria. The first criteria that a compression must meet is complete release; where complete release is defined as the minimum force between compression is less than 3 kg of force. Both the compression before and after each incomplete release were removed from our study. The second criteria applied to the compression was model fit, in order to evaluate the error in the model, a model error was calculated. The model error is the difference in the modeled force and the measured force squared normalized by the measured force, for the portion of the compression greater than 10 mm of depth. Any compression with an error more than 20 generated by the model was removed from our study. The third criteria a compression needs to meet was no energy generation. Several compressions appeared to have energy generation, which is defined as the force-depth loop crossing over upon itself at a depth greater than 10 mm. The fourth criteria was a minimum compression depth as well as a maximum decompression depth; where a qualifying compression must be at least 15 mm deep and the compression must not return to a depth less than -5mm where a positive depth is defined as going into the chest and a negative depth is defined as coming out of the chest.

In order to evaluate the model for the entire CPR event a trim mean, with trim of 10%, of each of the modeled characteristics was taken.

RESULTS

Nineteen events have been analyzed: the average age is 15 (Std Dev 4) years, and the average body mass is 48 (Std Dev 15) kg (Table 1). The average chest depth was 21 (Std Dev 9) cm and the average chest circumference was 85 (Std Dev 11) cm with a value not available for one event. The type of bed used during the CPR Event was also recorded: Electric Hospital Beds (including the Triadyne bed) were used in the eleven events that occur within the PICU, while the stretchers were use in the five events that occurred within the Emergency Department. Analysis of these data is ongoing and are too preliminary to present at this time. Our goal is

compare the stiffness and damping properties of the pediatric human with those of CPR manikins (Table 2)

Table 1: Event Characteristics

Event	Age	Body Mass	Chest Depth	Chest Circumference	Mattress / Bed Type	Backboard Type
	Years	kg	cm	cm		
AQCPR 1	16	55	20.3	101.6	Electric hospital bed	Crash Cart
AQCPR 2	16	55	20.3	101.6	Electric hospital bed	Crash Cart
AQCPR 3	13	45	14	74	Electric hospital bed	Crash Cart
AQCPR 4	22	25	26	76.5	Electric hospital bed	Crash Cart
AQCPR 5	10	40	15	71	Stryker Stretcher	Not available
AQCPR 6	16	45.5	16.5	87	Electric hospital bed	Crash Cart
AQCPR 7	12	45	17.8	76.2	Stryker Stretcher	Not available
AQCPR 8	14	50.25	16	83	Electric hospital bed	Crash Cart
AQCPR 9	15	67.5	18.8	77.5	Stretcher	Extrication
AQCPR 10	8	48	15	80.5	Electric hospital bed	Crash Cart
AQCPR 11	14.9	48	21	92	Electric hospital bed	Crash Cart
AQCPR 12 (B-D)	22.0	50	26	83	Triadyne	Crash Cart
AQCPR 13	19.0	80	50	105	Hausted Stretcher	Crash Cart
AQCPR 14	9.3	14.2	Not	Not available	Manual hospital bed	Crash Cart
AQCPR 15	13.0	40	17	75	Hausted Stretcher	Crash Cart
AQCPR 16	12.8	55	21	91	Electric hospital bed	Crash Cart
Mean	15	48	21	85		
Std Dev	4	15	9	11		
Max	22	80	50	105		
Min	8	14	14	11		

Table 2: Manikin Properties

Manikin	k_1 (N/m)	Std Dev (N/m)	k_2 (N/m²)	Std Dev (N/m²)	μ_1 (N·sec/m)	Std Dev (N·sec/m)	μ_2 (N·sec/m²)	Std Dev (N·sec/m²)
Resusci Junior	3866.5	174.8	25452.3	2304.6	-2.2	8.9	2589.1	243.4
Resusci Junior	4546.4	271.2	27964.1	5143.9	-1.0	8.7	2182.4	351.7
Resusci Junior	4308.0	273.5	7721.1	3774.1	5.4	8.0	2037.5	247.1
Resusci Junior	4440.2	231.8	3664.3	3690.5	17.4	7.8	1646.2	222.2
Mean	4290.3		16200.5		4.9		2113.8	
Std Dev	298.9		12288.7		9.0		389.5	
Resusci Anne	5315.8	223.9	465.0	2566.5	156.5	16.0	-516.4	338.2
Resusci Anne	4715.8	276.4	5278.1	2876.1	142.4	15.0	-358.5	282.2
Resusci Anne	5419.5	164.0	-2827.9	1773.6	141.7	13.6	-208.1	250.2
Resusci Anne	5388.6	372.6	-4862.7	3201.2	128.6	14.4	-93.7	281.4
Mean	5209.9		-486.9		142.3		-294.2	
Std Dev	332.3		4426.0		11.4		183.6	

ACKNOWLEDGEMENTS

This research was supported by grants from the US Department of Transportation, National Highway Traffic Safety Administration, and Laerdal Medical Corporation. The authors gratefully acknowledge the contributions of Mandip Kalsi and Dana Niles for their assistance in the testing.

REFERENCES

AASE, SO AND MYKLEBUST, H (2002). "Compression Depth Estimation for CPR Quality Assessment Using DSP on Accelerometer Signals." IEEE Transactions on Biomedical Engineering 49(3): 263-268.

ARBOGAST, KB, MALTESE, MR, et al. (2006). "Anterior-posterior thoracic force-deflection characteristics measured during cardiopulmonary resuscitation: comparison to post-mortem human subject data." Stapp Car Crash J 50: 131-45.

BANG, A., J. HERLITZ AND S. MARTINELL (2003). "Interaction between emergency medical dispatcher and caller in suspected out-of-hospital cardiac arrest calls with focus on agonal breathing. A review of 100 tape recordings of true cardiac arrest cases." Resuscitation 56: 25-34.

BOLTE JH IV. (2006) The Ohio State University. Personal Communication.

BOWMAN, F., J. MENEGAZZI, B. CHECK AND T. DUCKETT (1995). "The lower esophageal sphincter pressure during prolonged cardiac arrest and resuscitation." Ann Emerg Med 26: 216-219.

CHING RP, NUCKLEY DJ, HERSTED SM, ECK MP, MANN FA, SUN EA. (2001) "Tensile mechanics of the developing cervical spine" 45th Stapp Car Crash Conference.

CLARK, J., M. LARSEN, L. CULLEY, J. GRAVES AND M. EISENBERG (1992). "Incidence of agonal respirations in sudden cardiac arrest." Ann Emerg Med 21: 1464-1467.

HILKER CE, YOGANANDAN N, PINTAR FA. (2002) "Experimental determination of adult and pediatric neck scale factors." 46th Stapp Car Crash Conference.

IRWIN A AND MERTZ HJ. (1997) Biomechanical Basis for the CRABI and Hybrid III Child Dummies. 41st Stapp Car Crash Conference. SAE Paper No. 973317.

KENT, R, LESSLEY, D, et al. (2004). "Thoracic response to dynamic, non-impact loading from a hub, distributed belt, diagonal belt, and double diagonal belts." Stapp Car Crash J 48: 495-519.

KENT, R., D. LESSLEY AND C. SHERWOOD (2004). "Thoracic response to dynamic, non-impact loading from a hub, distributed belt, diagonal belt, and double diagonal belt." Stapp Car Crash Journal 48: 495-519.

KROELL, C, SCHNEIDER, D, et al. (1974). Impact tolerance and repsonse of the human thorax II. 18th Stapp Car Crash Conference.

NATIONAL HIGHWAY TRAFFIC SAFETY ADMINISTRATION. "Traffic Safety Facts 2004 – Children" US Department of Transportation, Report No DOT HS 809 906.

OUYANG J, ZHU Q, ZHAO W, XU Y, CHEN W, ZHOUG S. (2005) "Biomechanical Assessment of the Pediatric Cervical Spine Under Bending and Dynamic Loads" Spine Vol. 30 No. 24, pp E716-E723.

PRANGE, M (2006) Personal Communication

SCHEUER L AND BLACK S. (2000) “Developmental Juvenile Osteology” Academic Press.

VAN RATINGEN MR, TWISK D, SCHROOTEN M, BEUSENBERG MC. (1997) “Biomechanically Based Design and Performance Targets for a 3-Year Old Child Crash Dummy for Frontal and Side Impact” 41st Stapp Car Crash Conference. SAE Paper No. 973316.

AUTHOR LIST

1. Thomas Castner
   Address
   Center for Injury Research and Prevention
   The Children's Hospital of Philadelphia
   3535 Market Street
   11th Floor, Suite 1150
   Philadelphia, PA 19104
   Phone
   215 828 9172
   E-mail
   castner@seas.upenn.edu

2. Kristy B. Arbogast
   Address
   Center for Injury Research and Prevention
   The Children's Hospital of Philadelphia
   3535 Market Street
   11th Floor, Suite 1150
   Philadelphia, PA 19104
   Phone
   215 590 3118
   E-mail
   arbogast@email.chop.edu

3. Vinay Nadkarni
   Address
   Department of Anesthesia and Critical Care
   The Children's Hospital of Philadelphia
   34th Street and Civic Center Boulevard
   Phone
   215-590-7430
   E-mail
   Nadkarni@email.chop.edu

4. Robert Sutton
    Address
        7C02
        34th Street and Civic Center Blvd
        Philadelphia, PA 19014
    Phone
        215-590-5881
    Email:
        suttonr@email.chop.edu

5. Akira Nishisaki
    Address
        CHOP Main Building 7S Rm 26,
        34th street and Civic Center Blvd.
        Philadelphia, PA 19104
    Phone
        215-590-5505
    Email
        nishisaki@email.chop.edu

6. Matthew R. Maltese
    Address
        The Children's Hospital of Philadelphia
        34th & Civic Center Boulevard
        3535 Center for Injury Research, 11th Floor
        Philadelphia, PA 19104
    Phone
        267-426-7025
    Email
        maltese@email.chop.edu